NASA TECHNICAL NOTE

NASA TN D-8129 c.1

TECH LIBRARY KAFB, NM
0133922

NASA TN D-8129

LOAN COPY: RETURN TO
AFWL TECHNICAL LIBRARY
KIRTLAND AFB, N. M.

A SIMPLIFIED ANALYTICAL SOLUTION FOR THERMAL RESPONSE OF A ONE-DIMENSIONAL, STEADY-STATE TRANSPIRATION COOLING SYSTEM IN RADIATIVE AND CONVECTIVE ENVIRONMENT

Hirotoshi Kubota

Ames Research Center
Moffett Field, Calif. 94035

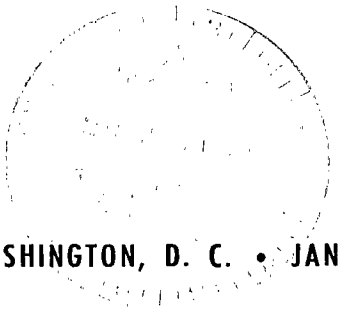

NATIONAL AERONAUTICS AND SPACE ADMINISTRATION • WASHINGTON, D. C. • JANUARY 1976

TECH LIBRARY KAFB, NM
0133922

1. Report No.	2. Government Accession No.	3. Recipient's Catalog No.
NASA TN D-8129		

4. Title and Subtitle
A SIMPLIFIED ANALYTICAL SOLUTION FOR THERMAL RESPONSE OF A ONE-DIMENSIONAL, STEADY-STATE TRANSPIRATION COOLING SYSTEM IN RADIATIVE AND CONVECTIVE ENVIRONMENT

5. Report Date
January 1976

6. Performing Organization Code

7. Author(s)
Hirotoshi Kubota

8. Performing Organization Report No.
A-6162

9. Performing Organization Name and Address
Ames Research Center, NASA
Moffett Field, Calif. 94035

10. Work Unit No.
506-16-41

11. Contract or Grant No.

12. Sponsoring Agency Name and Address
National Aeronautics and Space Administration
Washington, D. C., 20546

13. Type of Report and Period Covered
Technical Note

14. Sponsoring Agency Code

15. Supplementary Notes
National Research Council Associate at NASA Ames Research Center, Moffett Field, California, 94035, during the author's official leave from National Aerospace Laboratory of Japan.

16. Abstract

A simplified analytical method for calculation of thermal response within a transpiration-cooled porous heat shield material in an intense radiative-convective heating environment is presented. The essential assumptions of the radiative and convective transfer processes in the heat shield matrix are the "two-temperature" approximation and the specified radiative-convective heatings of the front surface. Sample calculations for porous silica with CO_2 injection are presented for some typical parameters of mass injection rate, porosity, and material thickness. The effect of these parameters on the cooling system is discussed.

17. Key Words (Suggested by Author(s))
Transpiration cooling
Radiative transfer
Heat and mass transfer
Material thermal response

18. Distribution Statement
Unclassified - Unlimited

STAR Category - 34

19. Security Classif. (of this report)	20. Security Classif. (of this page)	21. No. of Pages	22. Price*
Unclassified	Unclassified	36	$3.75

*For sale by the National Technical Information Service, Springfield, Virginia 22161

SYMBOLS

$\tilde{B}_o$	blowing parameter defined by equation (19)
C_H	heat transfer coefficient
C_p	specific heat
H	total enthalpy
$\tilde{H}$	convection coefficient parameter
h	volumetric convective heat transfer coefficient
I_e	external incident radiation intensity
I_R	radiation intensity outward in the matrix
I_T	radiation intensity transmitted inward in the matrix
K	absorption coefficient
k	thermal conductivity
L	thickness of the matrix
M	molecular weight
m,m'	index on radiation bands that penetrate the matrix
$\dot{m}$	mass injection rate
n,n'	index on radiation bands absorbed on the exposed surface
p	pressure
$\overline{p}$	normalized pressure
q	heat transfer rate
R	universal gas constant
S	scattering coefficient
T	temperature
t	time
U	velocity in x direction
x	distance from front surface

$\tilde{\alpha}$ viscous coefficient

$\tilde{\beta}$ inertial coefficient

ε emissivity

$\tilde{\varepsilon}$ relative error

η reflectivity

$\tilde{\eta}$ cooling effectiveness defined in equation (42)

θ normalized temperature

μ viscosity

ξ normalized spatial coordinate

ρ density

σ Stefan-Boltzmann constant

ϕ porosity

ψ_{con} convective heat transfer correction factor by mass injection (see eq. (17))

ψ_{rad} radiative heat transfer correction factor by mass injection (see eq. (20))

Subscripts:

b back face

cond conductive

e external

e edge of boundary layer

f fluid

i internal

o without injection

r radiative

radin incident radiative

rerad reradiative

s solid

w wall

∞ free stream

ν the νth spectral band of radiation

Superscripts:

$( )'$ differentiation with respect to ξ

A SIMPLIFIED ANALYTICAL SOLUTION FOR THERMAL RESPONSE OF A ONE-DIMENSIONAL, STEADY-STATE TRANSPIRATION COOLING SYSTEM IN RADIATIVE AND CONVECTIVE ENVIRONMENT

Hirotoshi Kubota*

Ames Research Center

SUMMARY

A simplified analytical method for calculation of thermal response within a transpiration-cooled porous heat shield material in an intense radiative-convective heating environment is presented. The essential assumptions of the radiative and convective transfer processes in the heat shield matrix are the "two-temperature" approximation and the specified radiative-convective heatings of the front surface. Sample calculations for porous silica with CO_2 injection are presented for some typical parameters of mass injection rate, porosity, and material thickness. The effect of these parameters on the cooling system is discussed.

INTRODUCTION

Probes entering the atmospheres of large planets, such as Jupiter and Saturn, encounter severe radiative heat loads in addition to the usual convective heat loads. The ablating heat shields, both charring and subliming types, used in the past to protect probes from convective heating, may not be adequate for these additional heat loads. For such entries, ablators will have to be chosen to withstand both the radiative and the convective heating.

One method, which is now being developed to withstand the radiative and convective heat load, uses reflecting ablation heat shields (refs. 1-3). It should be noted, however, that certain ablators, for example, silica, which are effective in protecting against convective heat may not block radiative heat and may, in fact, increase the incident radiative heating at certain ablation rates (ref. 4).

Another method which can be easily adapted to withstand the radiative and convective heat loads is a transpiration cooling technique. By choosing a porous heat shield which has a high reflectivity, part of the radiative heat load can be reflected. By choosing an absorbing transpiration gas (ref. 5), part of the radiative heat load can be absorbed and the convective heat load can be blocked.

---

*National Research Council Associate at NASA Ames Research Center, Moffett Field, California, 94035, during the author's official leave from National Aerospace Laboratory of Japan.

Accurate predictions of heat and mass transfer in the porous media must be solved from the coupling of momentum and energy equations for fluid and energy equation for a solid matrix (ref. 6). Since the convective heat exchange between solid and fluid affects the temperature distributions of solid and fluid in the porous matrix, two basic techniques have been introduced. One is the "one-temperature" assumption, that solid and fluid temperatures are the same, for a large heat transfer or small mass transfer rate, such as is the case in charring ablation (refs. 7 and 8); the other is the "two-temperature" assumption, that solid and fluid temperatures are not the same, an assumption that is essential for a small heat transfer and a large mass transfer rate (ref. 9).

In this investigation, the transpiration cooling system is studied theoretically with the intent of finding simple analytical solutions. This involves the interactions of the heat and mass transfer process within the porous heat shield. For this purpose, a simplified, one-dimensional, steady-state case with constant properties will be investigated. It is expected that, from this simplified model, the essential features and the basic parameters that govern the transpiration cooling system can be found.

ANALYSIS

Physical Model and Assumptions

The physical model considered in this analysis is sketched in figure 1. A one-dimensional porous matrix of thickness L is exposed to the external convective and radiative heat fluxes. The present analysis considers the heat transfer process only within the porous matrix under the conditions of given convective and radiative heating at the front surface. The coolant gas is injected through the matrix from back to front surfaces.

The analysis makes the following major assumptions:

1. Steady-state transpiration

2. Solid and gas temperatures in the matrix not equal (two-temperature assumption)

3. Continuum model for the porous matrix (volume element is large with respect to individual pores)

4. No reversal flow (all injected gases flow toward the heated front surface)

5. Specified incident heating fluxes and constant back-face temperature

6. Constant thermal and optical properties (independent of temperature, pressure, and wavelength)

7. Neither chemical reactions between the porous matrix and the injected gas nor dissociation of the injected gas

8. Negligibly small energy change due to the pressure difference in the porous matrix in comparison with other energy terms

9. Front surface impermeable to the external gas

Simplified Governing Equations

The complete transient differential equations, describing the conservations of mass, momentum, and energy without radiation in the porous matrix and with mass transfer, are presented in reference 10. By adding a radiative transfer term to the energy equation, the differential equations can be applied to the case with radiation. This radiative transfer term will be derived in the next section. The complete equations will not be presented here. The simplified equations, obtained by applying the previous assumptions, are as follows.

For fluid:

Mass conservation

$$\frac{d\dot{m}}{dx} = 0 \tag{1}$$

Momentum conservation - Darcy's equation

$$-\frac{dp_f}{dx} = \tilde{\alpha}\mu_f U_f + \tilde{\beta}\rho_f |U_f| U_f \tag{2}$$

Energy conservation

$$k_f \frac{d^2 T_f}{dx^2} + C_{p_f} \dot{m} \frac{dT_f}{dx} + \frac{h}{\phi}(T_s - T_f) - \frac{dq_r}{dx} = 0 \tag{3}$$

Perfect gas law

$$p_f = \rho_f \frac{R}{M_f} T_f \tag{4}$$

For solid:

Energy conservation

$$k_s \frac{d^2 T_s}{dx^2} - \frac{h}{1 - \phi}(T_s - T_f) - \frac{dq_r}{dx} = 0 \tag{5}$$

where $\tilde{\alpha}$, $\tilde{\beta}$, and ϕ are constants that depend on the porosity, and h is a volumetric heat transfer coefficient between solid and fluid and can be

written by the experimental correlation (ref. 11) as

$$h = 0.00434(C_{p_f}k_f^2)^{0.333}\mu_f^{-0.227}\dot{m}^{0.56}(\tilde{\alpha}/\tilde{\beta})^{1.44} \tag{6}$$

From equation (1) one obtains

$$\dot{m} = -\rho_f U_f = \text{constant} \tag{7}$$

that represents a given coolant injection rate at the back face. From equations (2), (4), and (7), one also obtains

$$p_f \frac{dp_f}{dx} = (\tilde{\alpha}\mu_f + \tilde{\beta}\dot{m})\dot{m}(R/M_f)T_f \tag{8}$$

Then, equations (3), (5), and (8) become a set of the governing equations.

Radiative transfer term, dq_r/dx.- The matrix material is partially transparent to radiation so that a part of the incident radiative flux penetrates the material to be backscattered in depth and the rest is absorbed at the surface (see fig. 2). The incident radiation is defined (ref. 2) as

$$q_{r_e} = \sum_{\nu=m}^{m'} q_{r_{e_\nu}} + \sum_{\nu=n}^{n'} q_{r_{e_\nu}} \tag{9}$$

where the first sum is radiation that penetrates and the last is surface absorbed radiation.

Thus, the radiative flux within the matrix q_r should be evaluated under the influence of the penetrating incident radiative flux $\sum_{\nu=m}^{m'} q_{r_{e_\nu}}$; hence, by the "two-flux" method described in appendix A, it is written as

$$q_r = \sum_{\nu=m}^{m'} q_{r_{e_\nu}} = \sum_{\nu=m}^{m'} \pi(I_{T_\nu} - I_{R_\nu}) \tag{10}$$

The radiative terms in equations (3) and (5) are then expressed, from the solution of the Kubelka-Munk equations (A1) and (A2), by

$$\frac{dq_r}{dx} = \sum_{\nu=m}^{m'} \pi\left(\frac{dI_{T_\nu}}{dx} - \frac{dI_{R_\nu}}{dx}\right) = -\sum_{\nu=m}^{m'} \pi K(I_{T_\nu} + I_{R_\nu}) \tag{11}$$

$$= -2\left(\frac{A_0}{A_1}\right)e^{\alpha x_K}\sum_{\nu=m}^{m'} q_{r_{e_\nu}} + 2\left(\frac{B_0}{B_1}\right)e^{-\alpha x_K}\sum_{\nu=m}^{m'} q_{r_{e_\nu}} \tag{12}$$

Boundary conditions.- Boundary conditions required for the simplified governing equations are (see fig. 3)

at $x = 0$;

$$-k_s \frac{dT_s}{dx} = q_w + q_{radin} - q_{rerad} \tag{13}$$

$$k_f \frac{d^2T_f}{dx^2} = 0 \quad \text{or} \quad -k_f \frac{dT_f}{dx} = 0 \tag{14}$$

$$p_f = p_{f_w} \tag{15}$$

at $x = L$;

$$T_s = T_f = T_b \tag{16}$$

where the convective heating rate with blowing (ref. 12), the incident radiative heating flux with blowing[1] and the surface reradiation heat flux are defined as

$$q_w = \rho_e U_e C_{H_O} \psi_{con} (H_e - H_w) = q_{w_O} \psi_{con} \tag{17}$$

$$\psi_{con} = \frac{\tilde{B}_O}{e^{\tilde{B}_O} - 1} \tag{18}$$

$$\tilde{B}_O = \frac{\dot{m}}{\rho_e U_e C_{H_O}} \tag{19}$$

$$q_{radin} = \sum_{\nu=n}^{n'} (1 - \eta_e) q_{r_{O_\nu}} \psi_{rad} \tag{20}$$

$$q_{rerad} = \varepsilon \sigma T_{s_w}^4 \tag{21}$$

In equations (17) and (20), ψ_{con} and ψ_{rad} are the correction factors for incident convective and radiative fluxes by mass injection, respectively.

Nondimensional Governing Equations and Boundary Conditions

The simplified equations (3), (5), and (8) can be written in the nondimensional forms as follows:

$$\theta_s'' + \Phi_1 (\theta_s - \theta_f) + \Phi_4 e^{\alpha L \xi} + \Phi_5 e^{-\alpha L \xi} = 0 \tag{22}$$

[1]Private communication with J. T. Howe.

$$\theta_f'' + \Phi_2\theta_f' + \Phi_3(\theta_s - \theta_f) + \Phi_6\, e^{\alpha L\xi} + \Phi_7\, e^{-\alpha L\xi} = 0 \tag{23}$$

$$\bar{p}_f\bar{p}_f' - \Phi_8\theta_f - \Phi_9 = 0 \tag{24}$$

where

$$\theta_s \equiv \frac{T_s - T_b}{T_{s_w} - T_b} \tag{25}$$

$$\theta_f \equiv \frac{T_f - T_b}{T_{s_w} - T_b} \tag{26}$$

$$\bar{p}_f \equiv \frac{p_f}{p_{f_w}} \tag{27}$$

$$\xi \equiv \frac{x}{L} \tag{28}$$

$$\left.\begin{aligned}
\Phi_1 &= -hL^2/k_s(1 - \phi) \\
\Phi_2 &= \dot{m}C_{p_f}L/k_f \\
\Phi_3 &= hL^2/k_f\phi \\
\Phi_4 &= 2KL^2(A_0/A_1)\sum_{\nu=m}^{m'} q_{r_e}{}_{\nu}/k_s(T_{s_w} - T_b) \\
\Phi_5 &= -(A_1B_0/A_0B_1)\Phi_4 \\
\Phi_6 &= (k_s/k_f)\Phi_4 \\
\Phi_7 &= -(k_s/k_f)(A_1B_0/A_0B_1)\Phi_4 \\
\Phi_8 &= L\dot{m}(R/M_f)(T_{s_w} - T_b)(\tilde{\alpha}\mu_f + \tilde{\beta}\dot{m})/p_{f_w}^2 \\
\Phi_9 &= T_b\Phi_8/(T_{s_w} - T_b)
\end{aligned}\right\} \tag{29}$$

( )' : differentiation with respect to ξ

The corresponding boundary conditions (eqs. (13) through (16)) are

at $\xi = 0$;

$$\theta_s(0) = 1 \tag{30}$$

$$\theta_s'(0) = \Phi_{10}(q_w + q_{radin} - q_{rerad}) \tag{31}$$

where

$$\Phi_{10} = -L/k_s(T_{s_w} - T_b) \tag{32}$$

$$\theta_f''(0) = 0 \tag{33}$$

or

$$\theta_f'(0) = 0 \tag{34}$$

$$\overline{F}_f(0) = 1 \tag{35}$$

at $\xi = 1$;

$$\theta_s(1) = 0 \tag{36}$$

$$\theta_f(1) = 0 \tag{37}$$

In equation (31), q_w, q_{radin}, and q_{rerad} are functions of only the surface temperature, T_{s_w}.

Method of Solution

General solutions of equations (22) and (23) can be written as

$$\theta_s(\xi) = \left(\sum_{k=1}^{3} c_k e^{\delta_k \xi} + c_o\right) + E_1 e^{\alpha L \xi} + E_2 e^{-\alpha L \xi} \tag{38}$$

$$\theta_f(\xi) = \left(\sum_{k=1}^{3} \gamma_k c_k e^{\delta_k \xi} + \gamma_o c_o\right) + E_3 e^{\alpha L \xi} + E_4 e^{-\alpha L \xi} \tag{39}$$

where the bracketed terms are the homogeneous solutions and the other terms are the particular solutions.

Coefficient δ_k in equations (38) and (39) is obtained from the homogeneous solutions of equations (22) and (23) as discussed in appendix B. The other coefficients are obtained from the boundary conditions, equations (30) through (37). Note that all coefficients except δ_k are implicit functions of T_{s_w}. The T_{s_w} value is determined by iteration to satisfy the energy balance given by equation (31) and equation (38) for $\xi = 0$, that is,

$$\theta_s'(0) = \sum_{k=1}^{3} c_k \delta_k + E_1 \alpha L - E_2 \alpha L \tag{40}$$

The pressure variable $\overline{p}_f$ is solved from equation (24) by integrating $\theta_f(\xi)$ as follows:

$$\overline{p}_f{}^2(\xi) = 2\Phi_8\left[\sum_{k=1}^{3}(\gamma_k c_k/\delta_k)\left(e^{\delta_k\xi} - 1\right) + (E_3/\alpha L)\left(e^{\alpha L\xi} - 1\right)\right.$$

$$\left. -(E_4/\alpha L)\left(e^{-\alpha L\xi} - 1\right)\right] + 2(\gamma_o c_o\Phi_8 + \Phi_9)\xi + 1 \qquad (41)$$

Sample Calculations

The effect of radiation penetration into the porous matrix has been tested for two boundary conditions, corresponding to (1) no conduction heat of the fluid at the front surface and (2) zero derivative of the fluid conduction heat at the front surface. The following table shows four typical sample calculations considered in this analysis.

Case	Radiative penetration	Boundary condition
I-A	Without	$\theta_f''(0) = 0$
I-B	Without	$\theta_f'(0) = 0$
II-A	With	$\theta_f''(0) = 0$
II-B	With	$\theta_f'(0) = 0$

In this sample calculation, silica (SiO_2) and carbon dioxide (CO_2) are taken as porous matrix and transpirant gas, respectively. Detailed description of their thermal and optical properties are shown in appendix C.

The radiative and convective heat loads for this sample calculation are taken for a 15° Saturn entry (ref. 3) at t = 23.7 sec, corresponding to maximum radiative heat loads.

$$q_{r_o} = 216.70 \text{ cal/sec/cm}^2$$

$$p_e = 2.091 \text{ atm}$$

$$U_\infty = 2.86\times10^6 \text{ cm/sec}$$

$$\rho_e U_e C_{H_o} = 1.186\times10^{-2} \text{ gm/cm}^2\text{/sec}$$

$$H_e = 0.9685\times10^5 \text{ cal/gm}$$

The spectral radiative heating data for SiO_2 blowing can be broken into 20 groups whose wavelength ranges cover 0.0919 μ through 9.92 μ. (The exact incident heating for CO_2 injection may be also estimated by the use of some numerical computations such as RASLE CODE (ref. 4).) The incident radiations are combined into groups 1-3 (a part of infrared) and 17-20 (ultraviolet) that are absorbed at the surface of the silica; groups 4-16 penetrate into the matrix.[1]

RESULTS AND DISCUSSIONS

Typical sample solutions are presented for a mass injection rate of $\dot{m} = 0.1$ gm/cm^2/sec, $\psi_{rad} = 1.0$ and $\theta_f''(0) = 0$. The solid and fluid temperature distributions and the pressure distributions for these sample cases are shown in figure 4(a) through figure 4(d) for the porosity range from $\phi = 0.2$ to $\phi = 0.8$. As would be expected, temperature distributions T_s and T_f are sufficiently close to each other so that the "one-temperature" approximation will provide a good solution at the smaller porosity. However, the "two-temperature" method is required for higher porosity cases.

The effect of radiative transfer within the porous matrix on temperature and fluid pressure is presented in figure 5(a) for the same input and boundary condition as before, except for a porosity of $\phi = 0.4$. A significant difference in temperature between two cases, with and without radiation heat, is observed.

The effect of boundary condition (case A, $\theta_f''(0) = 0$; and case B, $\theta_f'(0) = 0$) on solid and fluid temperature distribution is shown in figure 5(b) for the same input conditions as in figure 5(a) except for a larger mass injection rate of $\dot{m} = 0.2$ gm/cm^2/sec. There is no significant effect of the boundary condition on the solution except in the vicinity of the front surface. Since the boundary condition, $\theta_f''(0) = 0$, is a more reasonable assumption (ref. 10), the remainder of the calculations will be made under this condition.

Figure 6 presents the cross-plot of wall temperatures and back-face pressure of fluid as a function of porosity for various radiation heat transfer correction factors ψ_{rad}. Variations of the blowing correction factor for the radiative heating ψ_{rad} with blowing parameter is given for SiO_2 and carbon ablation (ref. 4).

The significant reduction of fluid wall temperature due to the matrix porosity is noted, as well as larger separation of solid and fluid temperatures as the value of porosity increases.

The variations of solid surface temperature T_{s_w}, due to mass injection rate and porosity, are shown in figure 7(a). Note that T_{s_w} is not significantly affected by the change of porosity to a higher value ($\phi \geqq 0.4$). This effect can be also recognized partly from figure 6.

---

[1]Private communication with J. T. Howe.

The cooling effectiveness is demonstrated in figure 7(b) for the various porosity and mass injection rate. The cooling effectiveness is defined by

$$\tilde{\eta} = \frac{T_{s_{w,o}} - T_{s_w}}{T_{s_{w,o}} - T_b} \Big/ \tilde{B}_o \tag{42}$$

where T_{s_w}, $T_{s_{w,o}}$, T_b, and $\tilde{B}_o$ are wall temperature with and without mass injection, back-face temperature, and injection parameter $\tilde{B}_o = \dot{m}/\rho_e U_e C_{H_o}$, respectively. The cooling effectiveness $\tilde{\eta}$ depends strongly on the mass injection rate, decreasing as the injection rate increases. However, the effect of porosity on cooling effectiveness, for a given mass injection rate, is not so significant; that is, the cooling effectiveness may be expressed in a single average curve (e.g., $\phi = 0.4$ case) that represents overall correlation between solid temperature, porosity, and mass injection rate.

The effect of material thickness on wall temperature and back-face heat conduction is shown in figure 8. The material thickness has an important effect on reducing back-face heat conduction but it has practically no effect on solid surface temperature.

The characteristics of the solutions, described above, can be plainly explained by using the concept of the convection coefficient parameter (ref. 13), $\tilde{H}$, defined by

$$\tilde{H} = \frac{hL}{\dot{m}C_{p_f}} \tag{43}$$

where h, the heat transfer coefficient, is inversely proportional to the matrix porosity. The parameter $\tilde{H}$, given by equation (43), signifies the degree of the heat exchange between the solid and fluid; that is, the larger the convection coefficient parameter (larger heat transfer coefficient or smaller porosity; larger matrix thickness or smaller mass injection rate, or both) the less difference there is between the solid and fluid temperatures.

The important criteria for a transpiration cooling system are cross-plotted in figure 9 with the assumption that the porous silica used for the present cooling system will melt at 1981 K (ref. 3). Then, the boundary criteria, in terms of radiation heat transfer correction factor ψ_{rad} and porosity limiting temperature, can be cross-plotted as in figure 9. In this figure, the region above each boundary curve requires ablation cooling while the other region requires only transpiration cooling. Also shown in the same figure is the functional curve, the ψ_{rad} vs $\dot{m}$ relation, obtainable from the external flow condition (ref. 4).

The cross points between the solid lines and the dashed line represent the minimum mass injection rate required for maintaining a porous material below the melting temperature. The higher porosity requires less mass injection rate for the given material thickness.

The thermal properties have important effects on the solutions. Figure 10 is a composite plot showing the effects of porosity, material thickness, and thermal properties on the front-surface solid and fluid temperatures. Nondimensionalized temperature differences for the solid and the fluid at the front surface, due to thermal properties (see appendix C), are defined as

$$\left.\begin{aligned} \tilde{\varepsilon}_{T_{s_w}} &= \frac{\left|T_{s_w}(\text{case } \langle a\rangle) - T_{s_w}(\text{case } \langle b\rangle)\right|}{T_{s_w}(\text{case } \langle a\rangle)} \\ \tilde{\varepsilon}_{T_{f_w}} &= \frac{\left|T_{f_w}(\text{case } \langle a\rangle) - T_{f_w}(\text{case } \langle b\rangle)\right|}{T_{f_w}(\text{case } \langle a\rangle)} \end{aligned}\right\} \tag{44}$$

respectively.

Note that the thermal properties for case <a> are selected at the melting temperature of silica, that is, 1981 K. For case <b>, the back-face temperature of 300 K is chosen. These are two extreme temperatures expected. Since $\tilde{\varepsilon}_{T_{s_w}}$ and $\tilde{\varepsilon}_{T_{f_w}}$ are the relative errors in temperature as a result of the thermal properties, the magnitude of these parameters shows the effect of the thermal properties. Note again, that the maximum effect is presented because the two extreme temperatures were taken.

The effect of the thermal properties is quite important on the solid wall temperature but not too important for the fluid wall temperature. The effect of porosity is to increase the temperature difference. The thinner material thickness is also strongly affected.

Finally, the present analytical solution has been compared with a more rigorous numerical solution (but still with constant thermal and optical properties) that retains the energy change term due to the pressure difference in the porous matrix (see assumption 8). The result shows that the present analysis compares within 1 percent of the rigorous solution, that is, the Adams-Moulton integral scheme. This result verifies the assumption that the term $U_f(dp_f/dx)$ can be neglected except for the case of extremely small porosity, that is, larger pressure drop within the porous matrix.

CONCLUDING REMARKS

A simplified analytical method for calculation of thermal response within a transpiration-cooled heat shield material in an intense radiative-convective heating environment is presented.

Essential features of the analysis are the "two-temperature" assumption, where matrix and flowing gas have different temperature distributions, and the specified radiative-convective heatings at the front surface.

Sample calculations for porous silica with CO_2 injection result in the following major conclusions:

1. Radiative transfer within the heat shield material increases the temperature of the material. Therefore, the absorption of radiation by transpirant gas does not play an effective role as a heat shield, but, the injection of the gas into the adjacent boundary layer reduces the incident heating and the temperature level within the matrix becomes lower (effect of ψ_{con} and ψ_{rad}).

2. Increasing the mass injection rate of the transpirant gas reduces temperature distributions, but increases the fluid pressure difference between front surface and back face. Cooling effectiveness per mass injection rate decreases as mass injection rate increases. In this respect, the behavior is similar to that of the general mass transfer cooling system.

3. Small porosity increases the volumetric heat transfer coefficient, thus causing closer temperature distributions between solid and fluid and resulting in higher back-face fluid pressure.

4. Increasing material thickness gives lower back-face heat conduction but has practically no effect on solid surface temperature.

5. The thermal conductivity and specific heat of the solid matrix have more important effects on the solutions than fluid thermal properties.

Agreement of the present solution with the more rigorous numerical calculation (the Adams-Moulton integral scheme) is quite good.

The calculated results were presented in the terms of the correlational form for mass injection rate, porosity, and radiation heat transfer correction factor, as the criteria for a transpiration cooling system.

Ames Research Center
National Aeronautics and Space Administration
Moffett Field, California 94035, September 16, 1975

APPENDIX A

RADIATIVE TRANSFER EQUATIONS

When the radiative emission inside the matrix is negligibly small compared to the radiant fluxes transmitted inward and backscattered outward, the one-dimensional radiation transfer can be described by the Kubelka-Munk "two-flux" equations (ref. 14) as

$$\frac{dI_{T_\nu}}{dx} = -(S + K)I_{T_\nu} + SI_{R_\nu} \tag{A1}$$

$$\frac{dI_{R_\nu}}{dx} = (S + K)I_{R_\nu} - SI_{T_\nu} \tag{A2}$$

where K and S are absorption coefficient and scattering coefficient, respectively, and are defined by

$$K = \phi K_f + (1 - \phi)K_s \tag{A3}$$

$$S = \phi S_f + (1 - \phi)S_s \tag{A4}$$

The boundary conditions for this set of simultaneous equations (A1) and (A2) are

at $x = 0$ (front surface);

$$I_{T_\nu} = (1 - \eta_e)I_{e_\nu} + \eta_i I_{R_\nu} \tag{A5}$$

at $x = L$ (back face);

$$I_{R_\nu} = \eta_b I_{T_\nu} \tag{A6}$$

as illustrated in figure 2.

The general solutions are

$$I_{T_\nu} = A(1 - \beta)e^{\alpha x} + B(1 + \beta)e^{-\alpha x} \tag{A7}$$

$$I_{R_\nu} = A(1 + \beta)e^{\alpha x} + B(1 - \beta)e^{-\alpha x} \tag{A8}$$

where

$$
\left.
\begin{aligned}
\alpha &= \sqrt{K(K + 2S)} \\
\beta &= \sqrt{K/(K + 2S)} \\
A &= (1 - \eta_e) I_{e_\nu} \frac{A_0}{A_1} \\
B &= -(1 - \eta_e) I_{e_\nu} \frac{B_0}{B_1} \\
A_0 &= [1 - \beta - \eta_b(1 + \beta)] e^{-\alpha L} \\
A_1 &= [(1 - \beta)^2 - (1 - \beta^2)(\eta_i + \eta_b) + (1 + \beta)^2 \eta_i \eta_b] e^{-\alpha L} \\
&\quad - [(1 + \beta)^2 - (1 - \beta^2)(\eta_i + \eta_b) + (1 - \beta)^2 \eta_i \eta_b] e^{\alpha L} \\
B_0 &= (1 - \beta^2)(1 + \eta_b^2) - 2(1 + \beta^2)\eta_b \\
B_1 &= A_0 A_1
\end{aligned}
\right\} \quad \text{(A9)}
$$

APPENDIX B

EXPRESSIONS FOR COEFFICIENTS IN SOLUTION

Characteristic Equation and Its Solution

By substituting the bracketed terms of equations (38) and (39) into the homogeneous forms of equations (22) and (23), one obtains

$$c_k\delta_k^2 + \Phi_1(c_k - \gamma_k c_k) = 0 \qquad (k = 1, 2, \ldots, k') \tag{B1}$$

$$\gamma_k c_k \delta_k^2 + \Phi_2 \gamma_k c_k \delta_k + \Phi_3(c_k - \gamma_k c_k) = 0 \qquad (k = 1, 2, \ldots, k') \tag{B2}$$

$$\gamma_o = 1 \tag{B3}$$

Then, since $c_k \neq 0$,

$$\gamma_k = (\delta_k^2 + \Phi_1)/\Phi_1 \qquad (k = 1, 2, \ldots, k') \tag{B4}$$

$$\delta_k^3 + \Phi_2\delta_k^2 + (\Phi_1 - \Phi_3)\delta_k + \Phi_1\Phi_2 = 0 \qquad (k = 1, 2, \ldots, k') \tag{B5}$$

and $k' = 3$. Therefore, δ_k are the roots of the characteristic equation

$$\delta^3 + \Phi_2\delta^2 + (\Phi_1 - \Phi_3)\delta + \Phi_1\Phi_2 = 0 \tag{B6}$$

Coefficients of Solutions for Case I-A and Case II-A

By substituting equations (38) and (39) into equations (22) and (23), one obtains

$$\left.\begin{aligned} E_1 &= -(a_2\Phi_6 + a_4\Phi_4)/(a_2a_3 + a_1a_4) \\ E_2 &= -(b_2\Phi_7 + b_4\Phi_5)/(b_2b_3 + b_1b_4) \\ E_3 &= (a_3\Phi_4 - a_1\Phi_6)/(a_2a_3 + a_1a_4) \\ E_4 &= (b_3\Phi_5 - b_1\Phi_7)/(b_2b_3 + b_1b_4) \end{aligned}\right\} \tag{B7}$$

where

$$\left.\begin{aligned} a_1 &= \alpha^2 L^2 + \Phi_1 \\ a_2 &= \Phi_1 \\ a_3 &= \Phi_3 \\ a_4 &= \alpha^2 L^2 + \Phi_2 \alpha L - \Phi_3 \\ b_1 &= \alpha^2 L^2 + \Phi_1 \\ b_2 &= \Phi_1 \\ b_3 &= \Phi_3 \\ b_4 &= \alpha^2 L^2 - \Phi_2 \alpha L - \Phi_3 \end{aligned}\right\} \tag{B8}$$

By applying the boundary conditions, equations (30), (33), (36), and (37), to equations (38) and (39)

$$c_1 = \begin{vmatrix} F_1 & A_2 & A_3 \\ F_2 & B_2 & B_3 \\ F_3 & C_2 & C_3 \end{vmatrix} \Big/ DET \tag{B9}$$

$$c_2 = \begin{vmatrix} A_1 & F_1 & A_3 \\ B_1 & F_2 & B_3 \\ C_1 & F_3 & C_3 \end{vmatrix} \Big/ DET \tag{B10}$$

$$c_3 = \begin{vmatrix} A_1 & A_2 & F_1 \\ B_1 & B_2 & F_2 \\ C_1 & C_2 & F_3 \end{vmatrix} \Big/ DET \tag{B11}$$

$$c_0 = 1 - E_1 - E_2 - c_1 - c_2 - c_3 \tag{B12}$$

where

$$DET = \begin{vmatrix} A_1 & A_2 & A_3 \\ B_1 & B_2 & B_3 \\ C_1 & C_2 & C_3 \end{vmatrix} \tag{B13}$$

$$A_k = 1 - e^{\delta_k} \qquad (k = 1, 2, 3) \tag{B14}$$

$$B_k = 1 - \gamma_k e^{\delta_k} \qquad (k = 1, 2, 3) \tag{B15}$$

$$C_k = \gamma_k \delta_k^2 \qquad (k = 1, 2, 3) \tag{B16}$$

For case II-A:

$$F_1 = 1 - E_1(1 - e^{\alpha L}) - E_2(1 - e^{-\alpha L}) \tag{B17}$$

$$F_2 = 1 - E_1 - E_2 + E_3 e^{\alpha L} + E_4 e^{-\alpha L} \tag{B18}$$

$$F_3 = -\alpha^2 L^2 (E_3 + E_4) \tag{B19}$$

For case I-A:

$$E_1 = E_2 = E_3 = E_4 = 0 \tag{B20}$$

Coefficients of Solutions for Case I-B and Case II-B

The boundary condition (33) of case I-A and case II-A is replaced by equation (34), therefore equations (B16) and (B19) should be replaced by

$$C_k = \gamma_k \delta_k \qquad (k = 1, 2, 3) \tag{B21}$$

$$F_3 = \alpha L(-E_3 + E_4) \tag{B22}$$

respectively.

APPENDIX C

THERMAL AND OPTICAL PROPERTIES OF POROUS MATRIX AND TRANSPIRANT GAS

Thermal and optical properties of porous silica and carbon dioxide used as the matrix and transpirant gas are given in tables 1 and 2.

TABLE 1 - PROPERTIES OF POROUS SILICA

Property	Value at		Dimension	Reference
	1981 K (case <a>)	300 K (case <b>)		
k_s	5.470×10^{-3}	2.157×10^{-3}	cal/sec/cm/K	3
C_{p_s}	0.309	0.172	cal/gm/K	3
ρ_s	1.49	1.49	gm/cm^3	3
K_s	0.001	0.001	cm^{-1}	3
S_s	40	40	cm^{-1}	3
n_e	0.06511	0.06511		3
n_i	0.17	0.17		3
n_b	0.8	0.8		3
ε	0.14	0.14		15

TABLE 2 - PROPERTIES OF CARBON DIOXIDE

Property	Value at		Dimension	Reference
	1981 K (case <a>)	300 K (case <b>)		
k_f	3.482×10^{-4}	2.387×10^{-5}	cal/sec/cm/K	12
C_{p_f}	0.327	0.202	cal/gm/K	16
K_f	0.1172	0.1172	cm^{-1}	17
S_f	0	0	cm^{-1}	17
μ_f	5.989×10^{-4}	1.500×10^{-4}	gm/cm/sec	12

Viscous Coefficient and Inertial Coefficient

Since the data for viscous coefficient $\tilde{\alpha}$ and inertial coefficient $\tilde{\beta}$ are not available for porous silica, the experimental correlations for porous feltmetal (ref. 9)

$$\tilde{\alpha} = 0.7336\times10^{9}\ (100\ \phi)^{-1.5378}\ (\mathrm{cm}^{-2})$$

$$\tilde{\beta} = 0.1517\times10^{4}\ (100\ \phi)^{0.2520}\ (\mathrm{cm}^{-1})$$

which are obtained from the extrapolated data, are used.

REFERENCES

1. Nachtscheim, P. R.; Peterson, D. L.; and Howe, J. T.: Reflecting and Ablating Heat Shields for Radiative Environments. AAS paper 71-147, also Advances in the Astronautical Sciences, vol. 29 II, 1971, pp. 253-264.

2. Howe, J. T.; Green, M. J.; and Weston, K. C.: Thermal Shielding by Subliming Volume Reflectors in Convective and Intense Radiative Environments. AIAA J., vol. 11, no. 7, 1973, pp. 989-994.

3. Howe, J. T.; and McCulley, L. D.: Volume-Reflecting Heat Shield for Entry Into the Giant Planet Atmospheres. AIAA Paper No. 74-669, 1974.

4. Nicolet, W. E.; Morse, H. L.; and Vojvodich, N. S.: Outer Planet Probe Entry Thermal Protection; Part I: Aerothermodynamic Environment. AIAA Paper No. 74-700, 1974.

5. Howe, J. T.: Shielding of Partially Reflecting Stagnation Surface Against Radiation by Transpiration of an Absorbing Gas. NASA TR R-95, 1961.

6. Curry, D. M.; and Cox, J. E.: Transient, Compressible Heat and Mass Transfer in Porous Media Using the Strongly Implicit Iteration Procedure. AIAA Paper No. 72-23, 1972.

7. Siegel, R.; and Goldstein, M. E.: Analytical Solution for Heat Transfer in Three-Dimensional Porous Media Including Variable Fluid Properties. NASA TN D-6941, 1972.

8. Kawamura, R.; and Nakajima, T.: Gasdynamic Study of Charring Ablation. Trans. Japan Soc. Aero. and Space Sci., vol. 14, no. 25, 1971, pp. 51-71.

9. Curry, D. M.; and Cox, J. E.: The Effect of the Porous Material Characteristics on the Internal Heat and Mass Transfer. ASME Paper 73-HT-49, 1973.

10. Curry, D. M.: Two-Dimensional Analysis of Heat and Mass Transfer in Porous Media Using the Strongly Implicit Procedure. NASA TN D-7608, 1974.

11. Schneider, P. J.; Maurer, R. E.; and Strapp, M. G.: Two-Dimensional Transpiration-Cooled Nosetip. J. Spacecraft & Rockets, vol. 8, no. 2, 1971, pp. 170-176.

12. Dorrance, W. H.: Viscous Hypersonic Flow. McGraw-Hill, New York, 1962.

13. Koh, J. C. Y.; and del Casal, E. P.: Heat and Mass Flow Through Porous Matrices for Transpiration Cooling. Proc. 1965 Heat Transfer and Fluid Mechanics Inst., 1965, pp. 263-281.

14. Kortüm, G.: Reflectance Spectroscopy. Springer-Verlag, New York, 1969.

15. Nicolet, W. E.; Howe, J. T.; and Mezines, S. A.: Outer Planet Probe Entry Thermal Protection; Part II: Heat-Shielding Requirements. AIAA Paper No. 74-701, 1974.

16. Obert, E. F.; and Gaggioli, R. A.: Thermodynamics. McGraw-Hill, New York, 1963.

17. Tien, C. L.: Thermal Radiation Properties of Gases. Advan. Heat Transfer, Academic Press, New York, vol. 5, 1968, pp. 253-324.

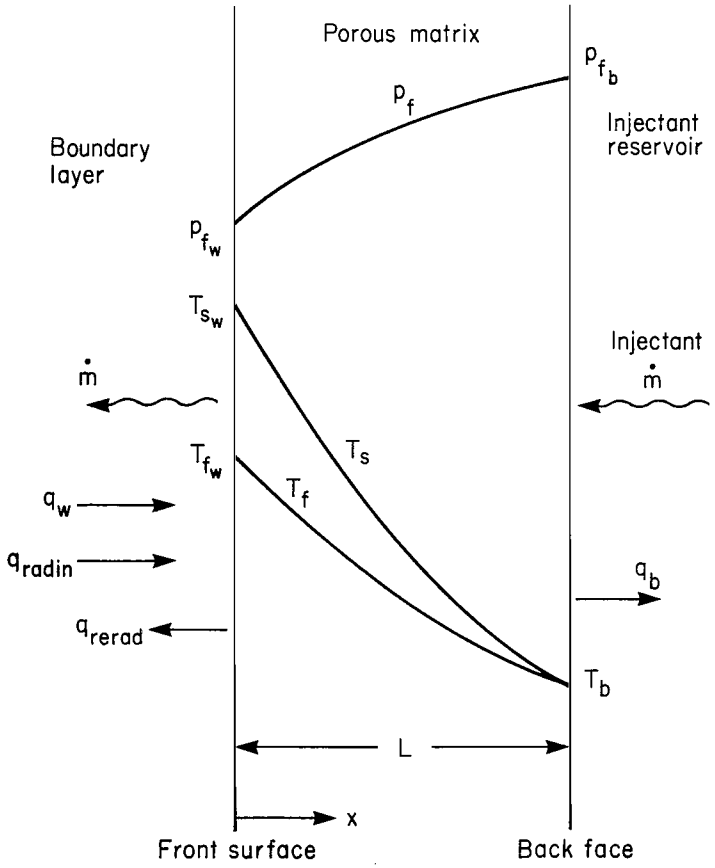

Figure 1.- Physical model.

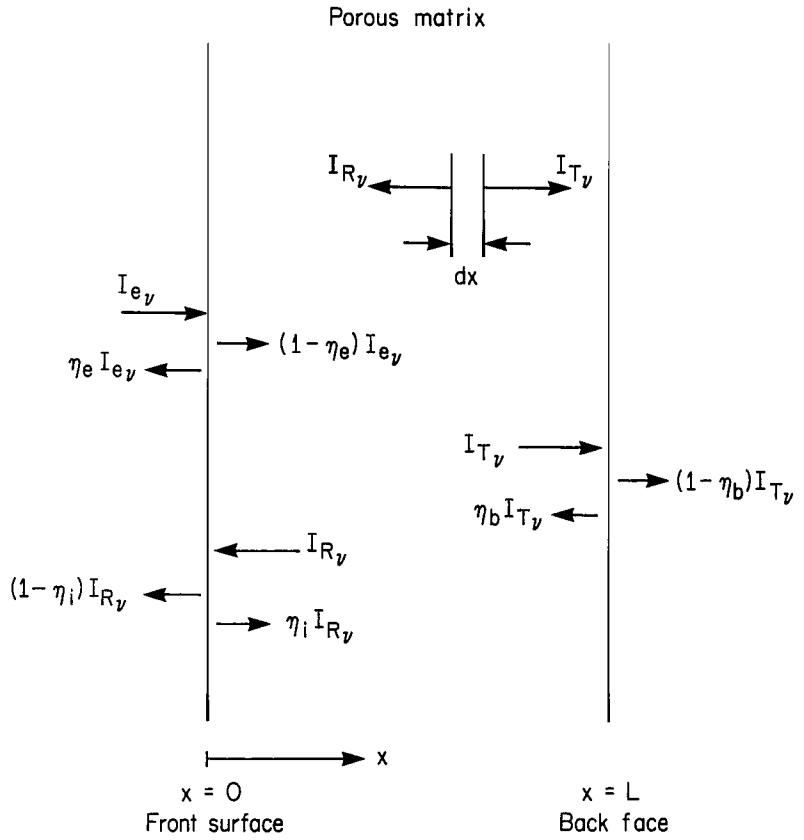

Figure 2.- Illustration of radiative transfer model.

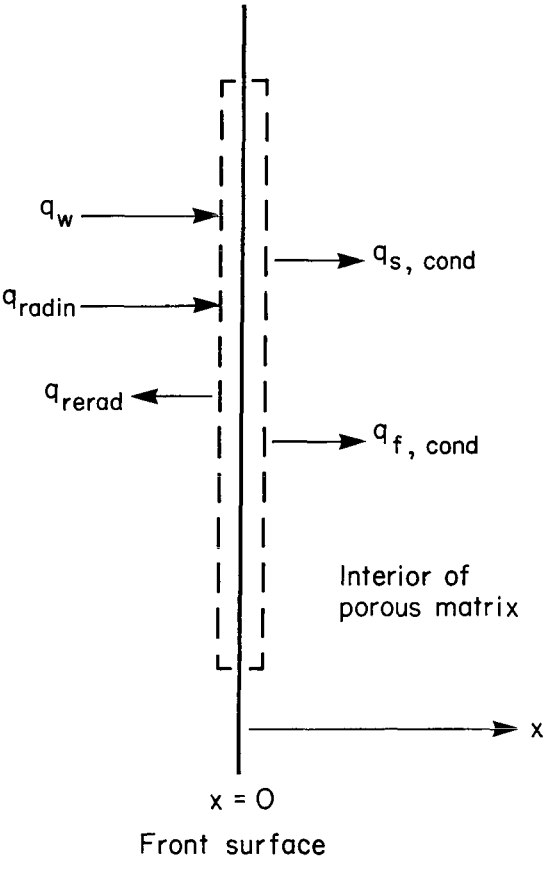

Figure 3.- Surface energy balance.

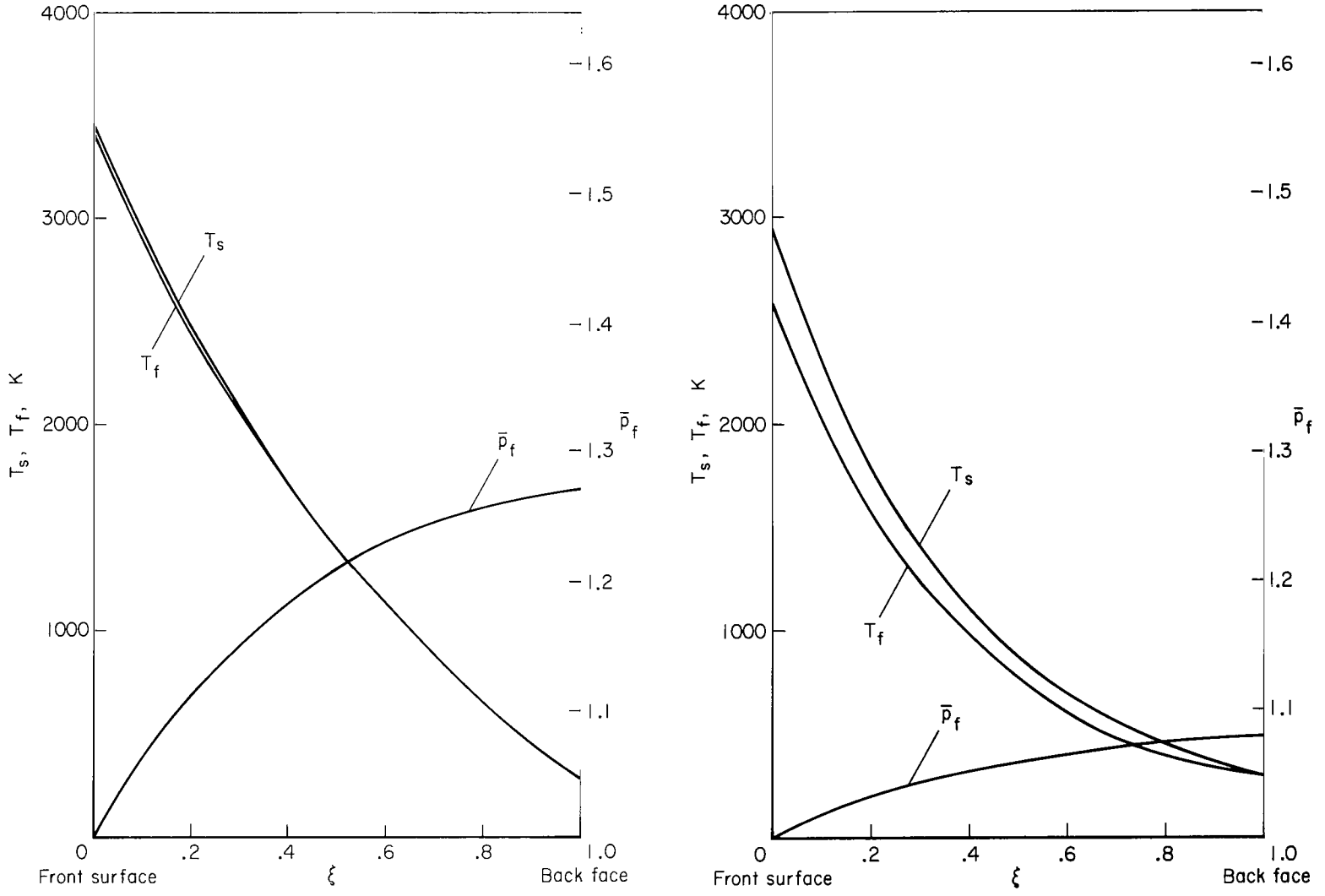

(a) ϕ = 0.2

(b) ϕ = 0.4

Figure 4.- Temperature and fluid pressure distributions within porous matrix: $\dot{m}$ = 0.1 gm/cm^2/sec, L = 1.0 cm, ψ_{rad} = 1.0, case II-A.

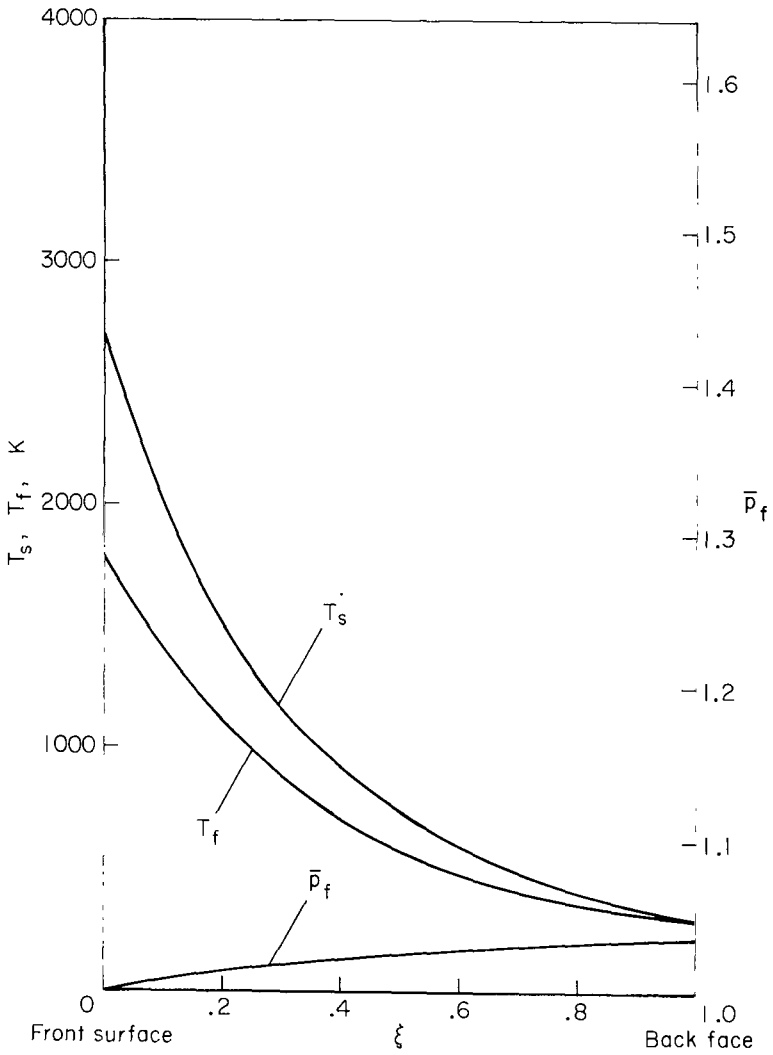

(c) ϕ = 0.6

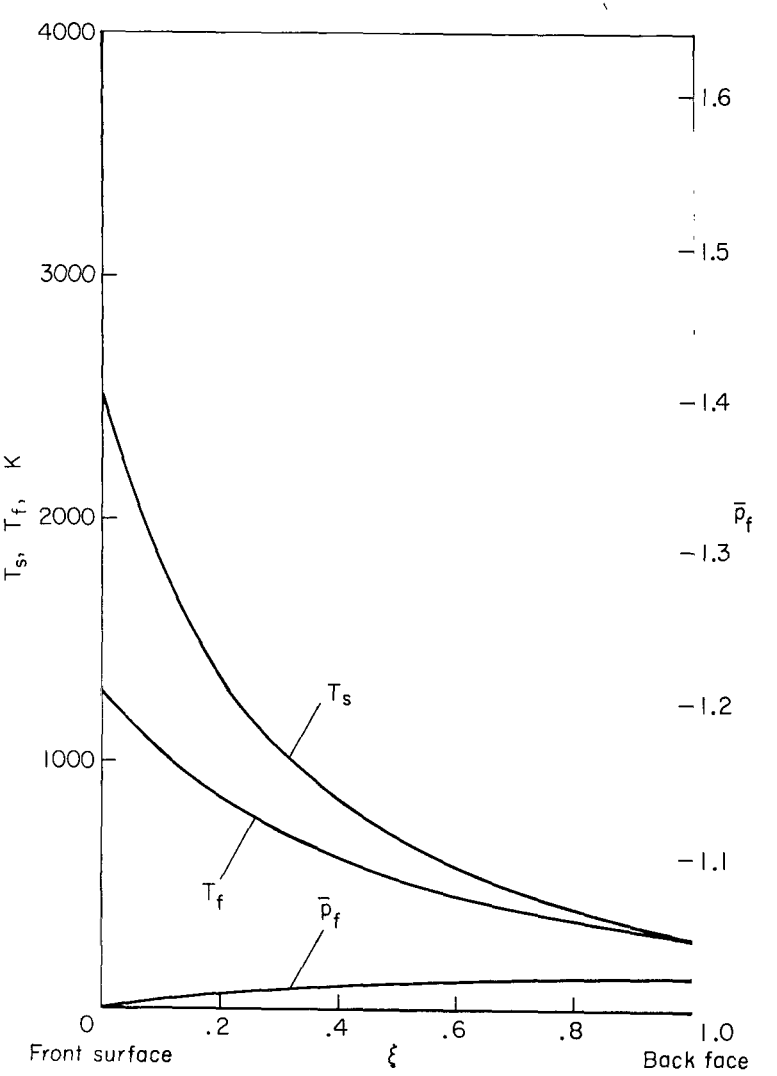

(d) ϕ = 0.8

Figure 4.- Concluded.

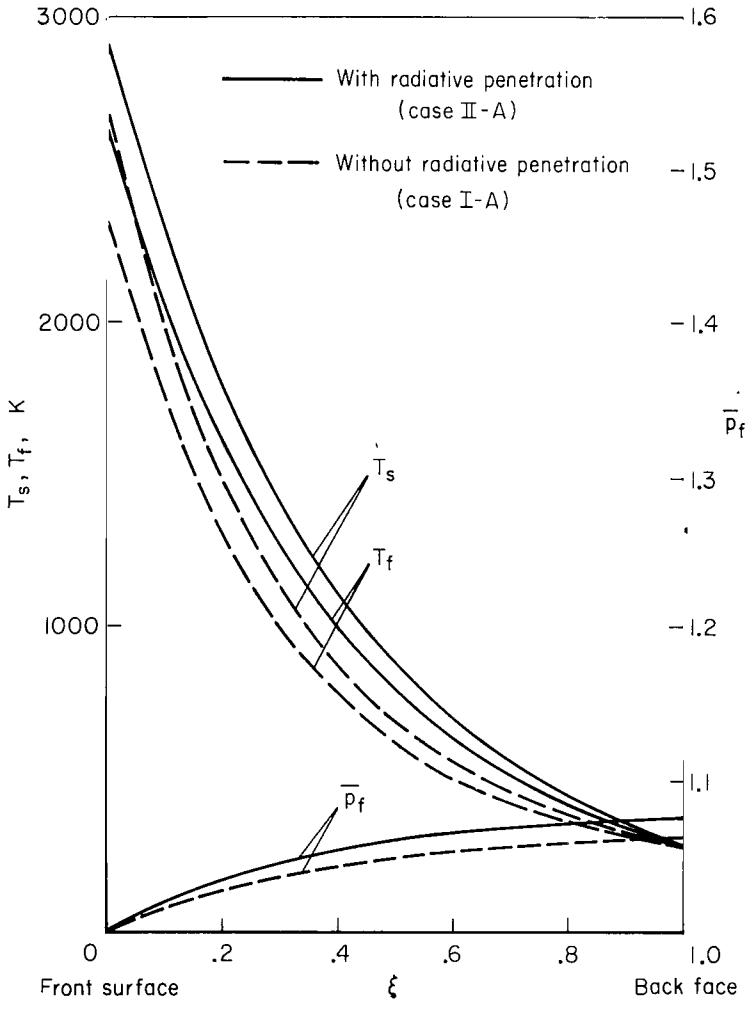

(a) Effect of radiative penetration for case A: $\dot{m}$ = 0.1 gm/cm^2/sec, L = 1.0 cm, ϕ = 0.4, ψ_{rad} = 1.0.

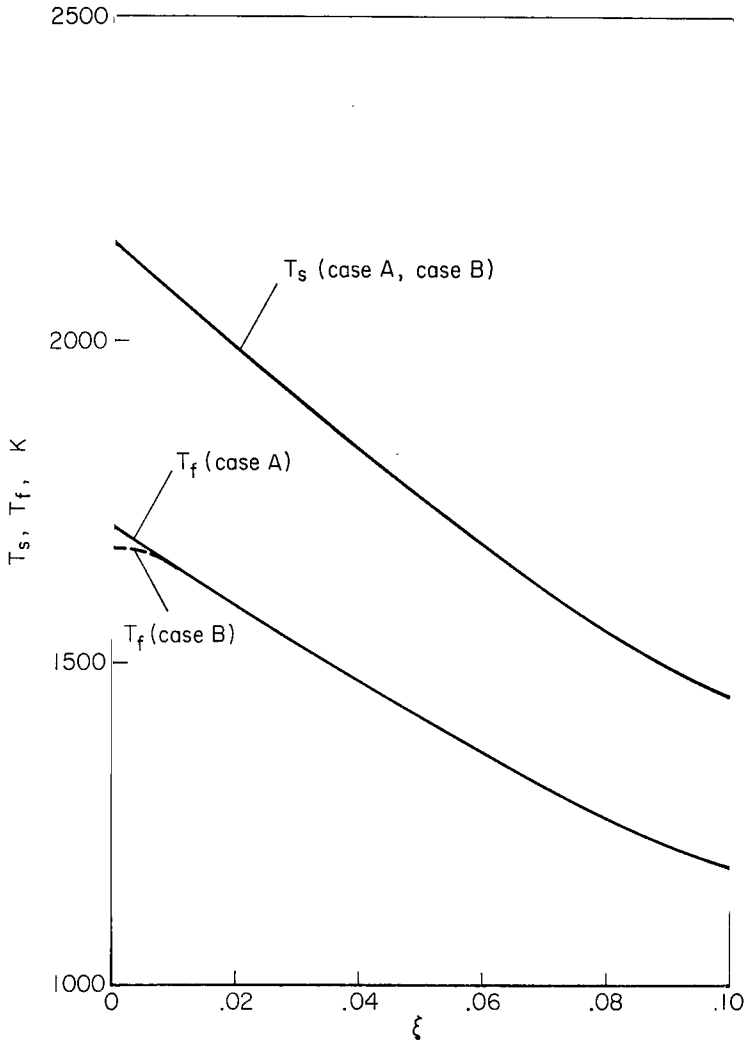

(b) Effect of boundary condition (with radiative penetration): $\dot{m}$ = 0.2 gm/cm^2/sec, L = 1.0 cm, ϕ = 0.4, ψ_{rad} = 1.0.

Figure 5.- Temperature and pressure distributions.

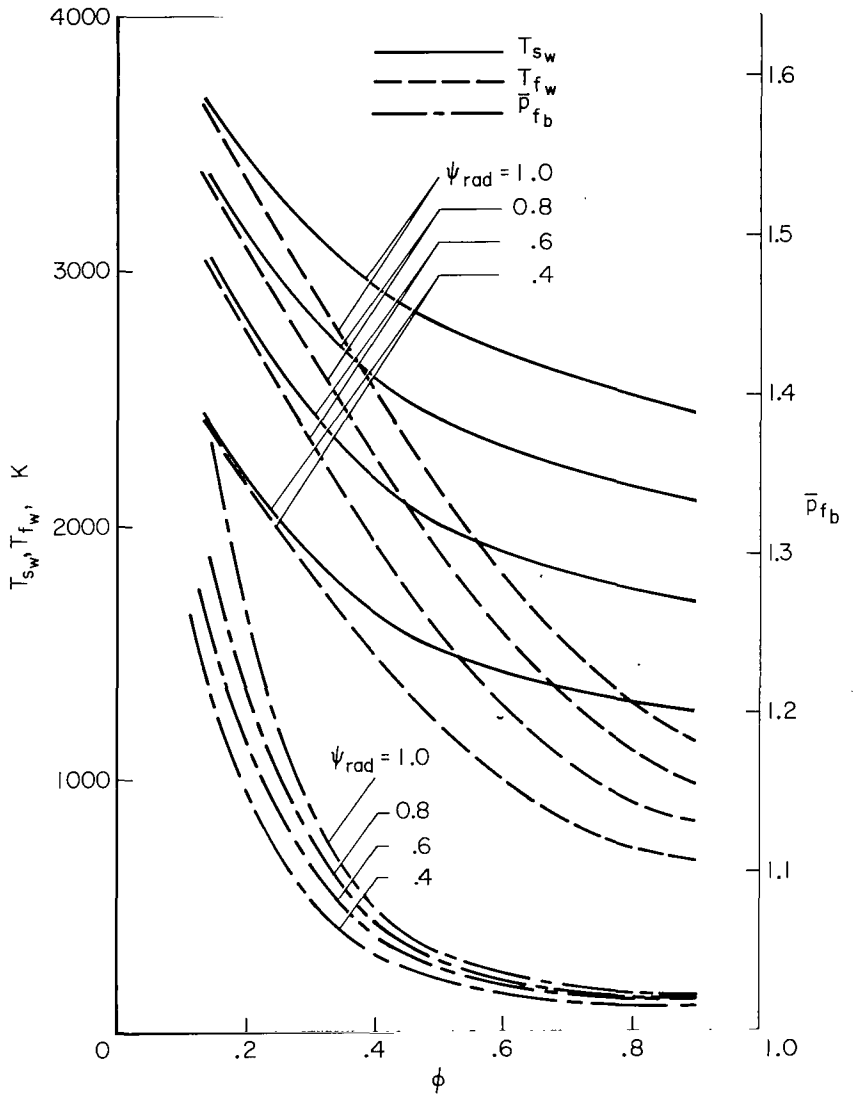

Figure 6.- Solid and fluid temperature variation at wall and fluid pressure at back face as a function of porosity: $\dot{m}$ = 0.1 gm/cm^2/sec, L = 1.0 cm, case II-A.

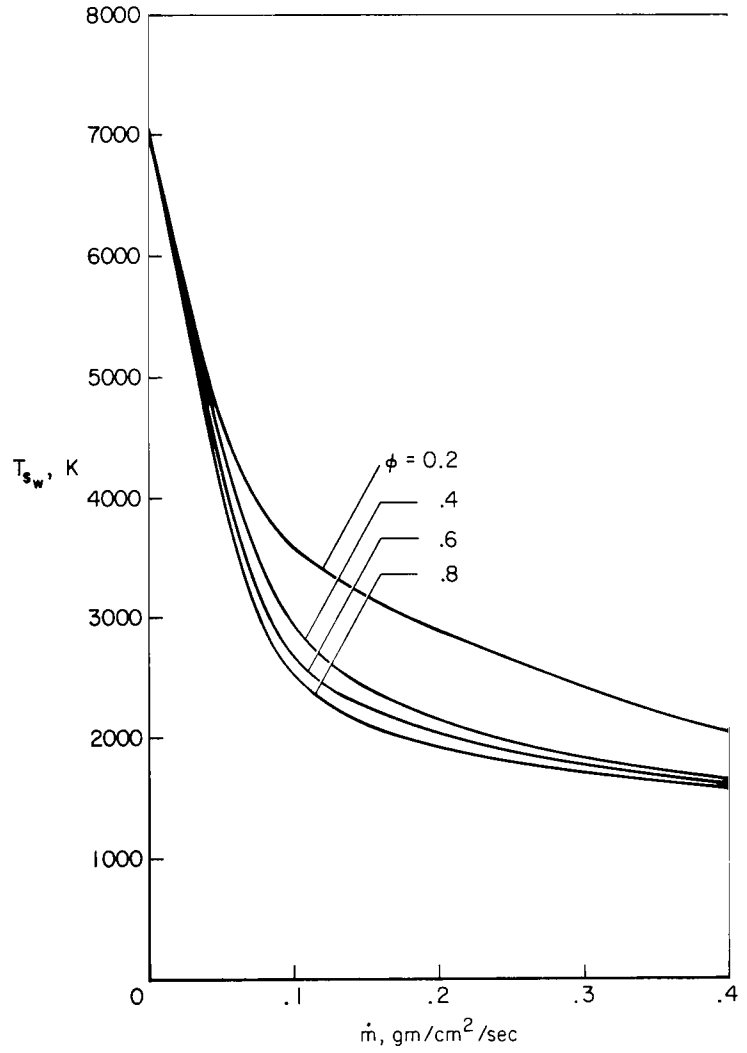

(a) Variation of solid surface temperature with mass injection rate.

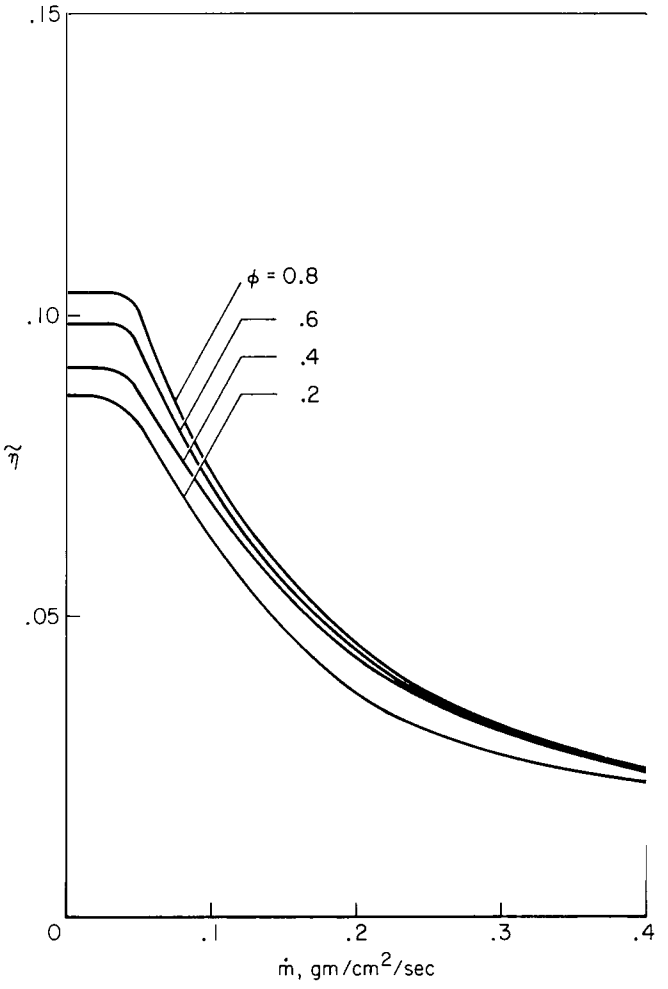

(b) Cooling effectiveness.

Figure 7.- Effect of mass injection rate: L = 1.0 cm, ψ_{rad} = 1.0, case II-A.

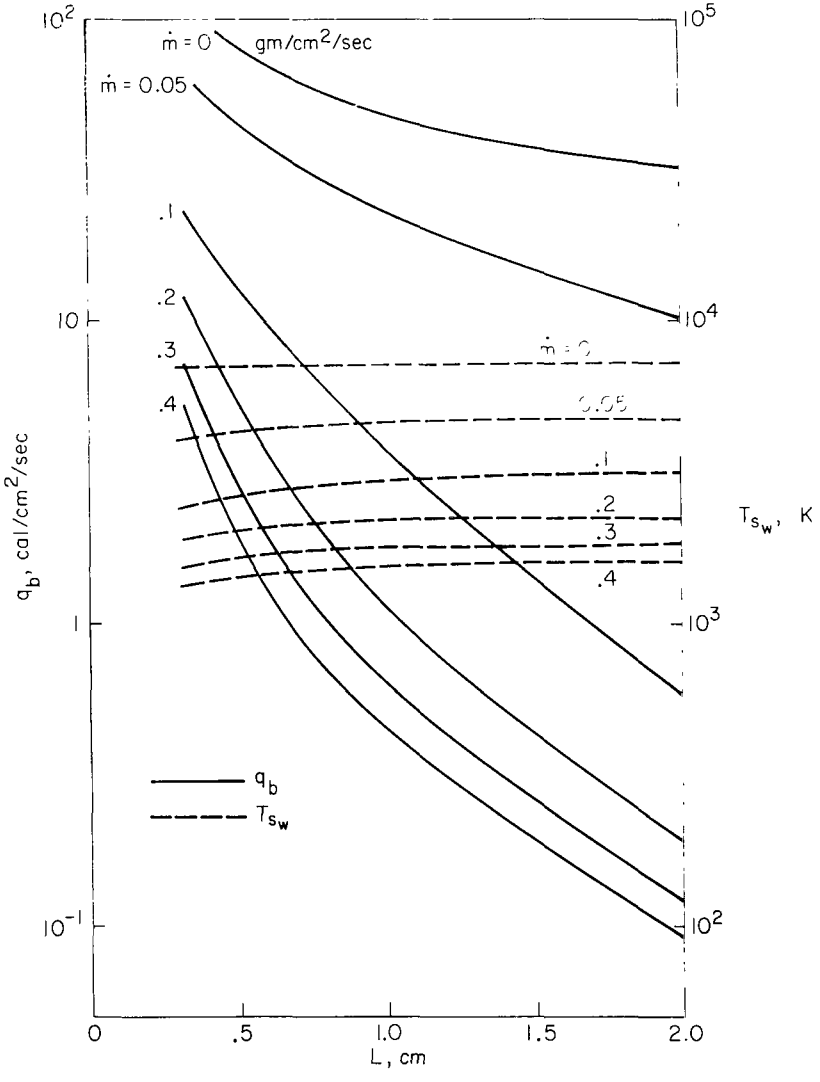

Figure 8.- Effect of material thickness; solid surface temperature and back-face heat conduction: ϕ = 0.4, ψ_{rad} = 1.0, case II-A.

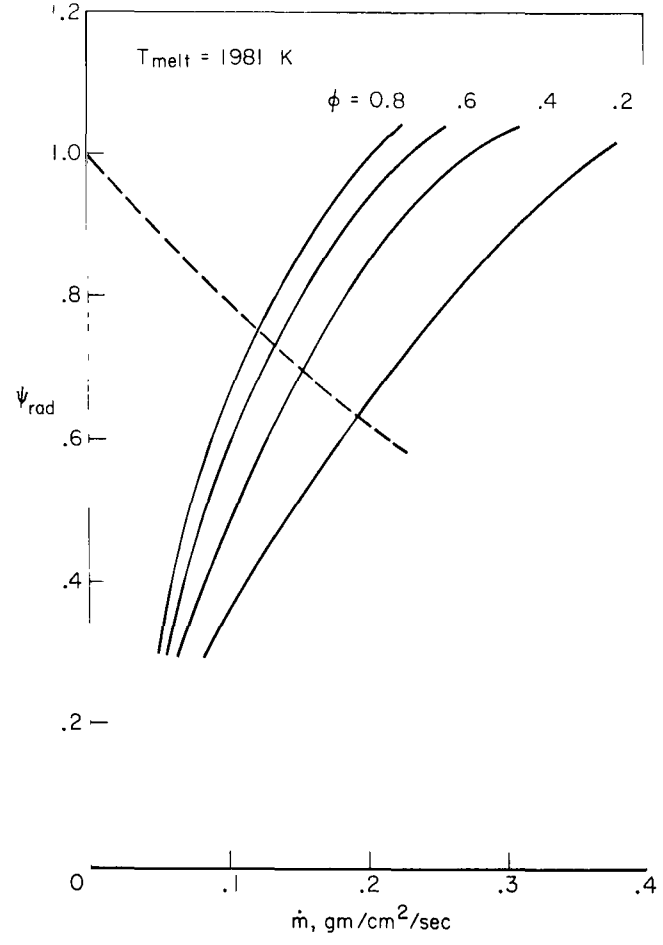

Figure 9.- Criteria for a transpiration cooling system (desired minimum mass injection rate): case II-A, L = 1.0 cm.

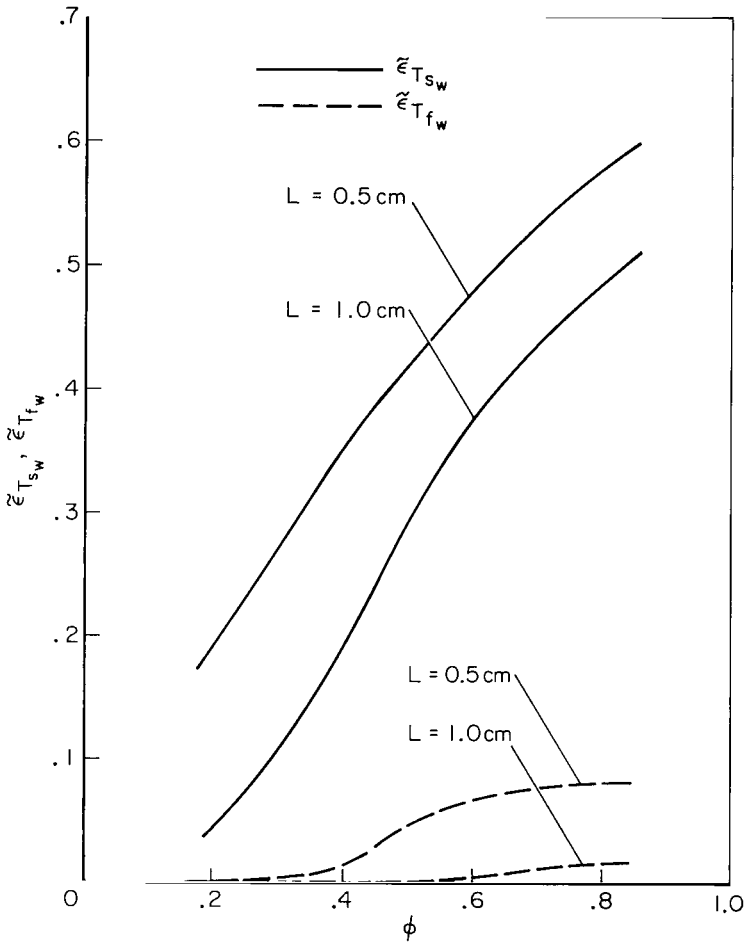

Figure 10.- Effect of thermal properties: $\dot{m}$ = 0.1 gm/cm^2/sec, ψ_{rad} = 1.0, case II-A.

NATIONAL AERONAUTICS AND SPACE ADMINISTRATION
WASHINGTON, D.C. 20546

OFFICIAL BUSINESS
PENALTY FOR PRIVATE USE $300

SPECIAL FOURTH-CLASS RATE BOOK

POSTAGE AND FEES PAID
NATIONAL AERONAUTICS AND SPACE ADMINISTRATION
451

U.S.MAIL

188 001 C1 U D 760109 S00903DS
DEPT OF THE AIR FORCE
AF WEAPONS LABORATORY
ATTN: TECHNICAL LIBRARY (SUL)
KIRTLAND AFB NM 87117

POSTMASTER: If Undeliverable (Section 158 Postal Manual) Do Not Return

"The aeronautical and space activities of the United States shall be conducted so as to contribute ... to the expansion of human knowledge of phenomena in the atmosphere and space. The Administration shall provide for the widest practicable and appropriate dissemination of information concerning its activities and the results thereof."

—NATIONAL AERONAUTICS AND SPACE ACT OF 1958

NASA SCIENTIFIC AND TECHNICAL PUBLICATIONS

TECHNICAL REPORTS: Scientific and technical information considered important, complete, and a lasting contribution to existing knowledge.

TECHNICAL NOTES: Information less broad in scope but nevertheless of importance as a contribution to existing knowledge.

TECHNICAL MEMORANDUMS: Information receiving limited distribution because of preliminary data, security classification, or other reasons. Also includes conference proceedings with either limited or unlimited distribution.

CONTRACTOR REPORTS: Scientific and technical information generated under a NASA contract or grant and considered an important contribution to existing knowledge.

TECHNICAL TRANSLATIONS: Information published in a foreign language considered to merit NASA distribution in English.

SPECIAL PUBLICATIONS: Information derived from or of value to NASA activities. Publications include final reports of major projects, monographs, data compilations, handbooks, sourcebooks, and special bibliographies.

TECHNOLOGY UTILIZATION PUBLICATIONS: Information on technology used by NASA that may be of particular interest in commercial and other non-aerospace applications. Publications include Tech Briefs, Technology Utilization Reports and Technology Surveys.

Details on the availability of these publications may be obtained from:

SCIENTIFIC AND TECHNICAL INFORMATION OFFICE

NATIONAL AERONAUTICS AND SPACE ADMINISTRATION

Washington, D.C. 20546